



HAL
open science

Investigation and properties of novel low melting glasses in the ternary system $\text{Sb}_2\text{O}_3\text{-PbO-Me}_2\text{O}_3$

Yasmina Taibi, Marcel Poulain, Messaoud Legouera, Alima Mebrek

► To cite this version:

Yasmina Taibi, Marcel Poulain, Messaoud Legouera, Alima Mebrek. Investigation and properties of novel low melting glasses in the ternary system $\text{Sb}_2\text{O}_3\text{-PbO-Me}_2\text{O}_3$. *International Journal of Applied Glass Science*, 2022, 13 (2), pp.254-262. 10.1111/ijag.16545 . hal-03516407

HAL Id: hal-03516407

<https://hal.science/hal-03516407v1>

Submitted on 25 Aug 2022

HAL is a multi-disciplinary open access archive for the deposit and dissemination of scientific research documents, whether they are published or not. The documents may come from teaching and research institutions in France or abroad, or from public or private research centers.

L'archive ouverte pluridisciplinaire **HAL**, est destinée au dépôt et à la diffusion de documents scientifiques de niveau recherche, publiés ou non, émanant des établissements d'enseignement et de recherche français ou étrangers, des laboratoires publics ou privés.

INVESTIGATION AND PROPERTIES OF NOVEL LOW MELTING GLASSES IN THE TERNARY SYSTEM $\text{Sb}_2\text{O}_3\text{-PbO-Me}_2\text{O}_3$

Y. Taibi^a, M. Poulain^b, M. Legouera^c, A. Mebrek^d

^a Laboratoire de Mines, Métallurgie et Matériaux, ENSMM-Annaba, Ex CEFOS-Sidi Amar, 2300 Annaba, Algérie

^b Sciences Chimiques, Université de Rennes 1, Campus Beaulieu, F-35042 Rennes, France

^c Dept Mécanique, Université de Skikda, 21000 Algérie

^d Research Center in Industrial Technology CRTI, P.O. Box 64, Cheraga 16014, Algiers, Algeria

Abstract

New glasses based on $\text{Sb}_2\text{O}_3\text{-PbO}$ association have been synthesized and characterized. The limits for glass formation have been investigated in ternary systems encompassing an oxide of IIIA group elements like Al_2O_3 , Ga_2O_3 and In_2O_3 as the third component. Fast quenching is required to prevent melt crystallization, which results in thin samples. Chemical analysis of elements shows a rather good agreement between nominal and analyzed compositions. Glass transition temperature, T_g , ranges between 255°C and 280°C , depending on composition. Density and hardness have been measured for typical composition.

Keywords

Lead antimony glass. Thermal properties. Density. Hardness

1. Introduction

The use of lead oxide as a significant glass component is older than modern chemistry and physics. In 1675 George Ravenscroft defined a new glass composition containing lead oxide, leading to larger working range in the molten state, reduced hardness and higher refractive index, which increases surface brightness [1, 2].

Heavy Metal Oxide Glasses (HMOG) make a family of special glasses that has been the subject of numerous studies. They may be roughly defined as glasses free of classical vitrifiers SiO_2 , B_2O_3 , P_2O_5 [3]. These glasses exhibit high refractive index, close to 2, large optical non-linearity and extended optical transmission in the infrared spectrum [4, 5, 6]. Among HMOG, germanate glasses appear as an intermediate group as GeO_2 is considered as a classical network former according to Zachariasen's rules [7], and also because their refractive index is somewhat lower.

1 Antimonite glasses based on Sb_2O_3 have attracted growing interest, mainly because numerous
2 glass forming systems have been identified so far, especially in polyanionic systems:
3 oxyhalides and oxysulfides. In addition their stability against devitrification may be very
4 large. Antimony oxide glasses have been reported in association to alkali oxides and in
5 multicomponent systems [8, 9, 10].
6

7 According to previous reports, $PbO-Sb_2O_3$ glasses exhibit good chemical durability and low
8 crystallization rates [11, 12]. Addition of the oxides of III A group elements like Al_2O_3 ,
9 Ga_2O_3 and In_2O_3 to the $PbO-Sb_2O_3$ based glass is likely to ameliorate their physical
10 properties. The choice of these oxides was based on the occurrence of a binary glass forming
11 range in combination to PbO . Table 1 reports the compositional limits of these binary glasses:
12
13

14 Table 1
15

M_2O_3	Maximum reported glass forming range (mol % PbO)
Al_2O_3	50-95 mol% PbO [13]; 67 – 95 mol% PbO [14]
Ga_2O_3	69 -81mol% PbO [15]; 58 -82 mol% PbO [16]; 57 - 82 mol% PbO [17];
In_2O_3	< 5 mol% PbO [18]

16
17
18
19
20
21

22 The aim of the present work is to explore new glass compositions in multicomponent systems
23 based on antimony oxide and to assess the potential of these glasses
24
25

26 2. Experimental 27

28 Materials used in this research are Sb_2O_3 (99,9%), PbO (99,9%), In_2O_3 (98%), Ga_2O_3 (98%),
29 and Al_2O_3 (98%) from Aldrich, WWR and Metal Europe. Glass samples were prepared using
30 the standard melt-quenching technique. Crystalline powders were intimately mixed in an
31 agate mortar. Then batch was heated up to melting in glass crucible for 5 min. Finally the
32 melts were cast and quenched between two brass plates to obtain a fast cooling rate close to a
33 few hundred K/S. In these conditions, sample thickness ranges between 0.8 and 1mm.
34
35

36 Main physical characterizations include X ray diffraction, thermal analysis microhardness and
37 density. X-ray diffraction patterns were obtained using $Cu K\alpha$ radiation on Philips PW1830
38 diffractometer. Differential scanning calorimetric measurements were performed on small
39 samples using a DSC 2010 from TA Instrument in aluminum sealed pans under N_2
40 atmosphere. Current heating rate was $10 K.min^{-1}$ and experimental error was $\pm 2^\circ C$ for glass
41 transition and onset of crystallization. Chemical composition was checked using Oxford Link
42 ISIS probe in a JEOL 6400 Scanning Electron Microscope dispersive γ -ray spectrometer
43 working at 20 KV. Density was measured using an ACCUPYC 1330 Micrometrics Helium
44 Picnometer with a precision of about $\pm 0,0005g/cm^3$. The samples were indented with
45 Matsuzawa MXT set-up. The value is averaged from 10 indentations or more, made on each
46 sample.
47
48
49
50

51 3. Results 52

53 3.1 Glass formation: 54

55 Our primary investigation of the binary Sb_2O_3-PbO based system confirms that the limits for
56 glass formation are extended, when faster quenching rates are used. These limits lie between
57 80 and 10% mol Sb_2O_3 as shown in Fig1.
58
59
60
61
62
63
64
65

Prepared glasses are stable at room atmosphere. At visual inspection, they appear transparent and yellow colored for glass samples between 80 and 40 mol % Sb_2O_3 . As PbO content increases, glass samples appear dark. This coloration arises from lead reduction: Indeed, as shown in figure 2, a metallic phase area corresponding to pure lead was observed in a dark glass sample. In practice, melt must be kept at room atmosphere for a longer time –e.g. 8 mn– to ensure oxidizing atmosphere.

In order to confirm glass composition, elemental analysis was performed for some samples with nominal composition $(100-x) \text{Sb}_2\text{O}_3.x\text{PbO}$ ($x= 50,60,70,80,90$). The analytical results reported in Table 2 show a rather good agreement between nominal and analyzed Sb concentration, while lead concentration is smaller than expected. Silicon content that arises from crucible increases as PbO concentration and melting time increase.

Table 2:

Acronym	mol %		Nominal composition			Analyzed composition			
	Sb_2O_3	PbO	Sb	Pb	O	Sb	Pb	O	Si
50 Sb_2O_3 50PbO	50	50	28.57	17.14	57.14	29.5	13.4	55.8	1.3
40 Sb_2O_3 60PbO	40	60	25	18.75	56.25	21.7	17.2	54.8	0.9
30 Sb_2O_3 70PbO	30	70	20.68	24.13	48.27	21.5	22.3	52.6	3.5
20 Sb_2O_3 80PbO	20	80	15.38	30.76	53.84	15.6	27.1	54.0	3.3
10 Sb_2O_3 90PbO	10	90	8.69	39.13	52.17	8.2	31.8	55.6	4.4

Glass formation has been investigated in various Sb_2O_3 -PbO- Me_2O_3 ternary systems, where $\text{Me} = \text{Al}, \text{In}, \text{Ga}$. Corresponding vitreous areas in nominal compositions are reported in fig3.

For all these systems, the experimental vitreous area is very narrow. For example, In_2O_3 content should not exceed 5 mol % while it may reach 15 mol % with Al_2O_3 and Ga_2O_3 . Sample color remains yellow fro the ternary glasses containing Al_2O_3 and Ga_2O_3 but it turns to green for the largest In_2O_3 contents.

3.2 X Ray Diffraction

The XRD patterns confirm the amorphous character of the samples, as shown in figure 4 for typical glass compositions. These patterns show a broad main peak at $2\Theta = 27,9^\circ$. Beyond this peak, a second one is observed at $2\Theta = 54^\circ$.

3.3 Thermal Properties:

3.3.1 Binary system

Differential Scanning Calorimetry has been implemented between 100 and 500°C. Typical DSC scans are reported in figure 5.

The evolution of the characteristic temperatures corresponding to glass transition (T_g), onset of crystallization (T_x) and exotherm maximum (T_p) versus concentration is plotted in figure 6(a) The stability factors S [19] and $\Delta T = T_x - T_g$ [20] that give an estimate of glass forming ability appears in figure 6(b). Glass transition varies between 255 and 276°C. As one could expect, characteristic temperatures depends on Sb_2O_3 content. These results suggest that glass stability against devitrification is maximum for high Sb_2O_3 concentration ($> 70\%$) and for

1 large lead concentration (90 % PbO). Intermediate compositions appear more prone to
2 devitrification.
3

4 **3.3.2 Ternary system**

5
6
7
8 For comparison, thermal measurements have been carried out on a set of three samples with
9 the same general, formula: $x \text{Sb}_2\text{O}_3 - (95-x) \text{PbO} - 5\text{Me}_2\text{O}_3$ (Me = Al, Ga, In, and $10 < x < 80$)

10 The composition dependence of glass transition temperature (T_g) is reported in fig 7. The
11 curves expressed the same behavior as observed in the binary system for glass transition: T_g
12 increases for large PbO concentrations ($> 40\%$). In a general way, T_g increases with ionic
13 radius ($\text{Al}^{3+} < \text{Ga}^{3+} < \text{In}^{3+}$).
14

15 We have also prepared samples with different In_2O_3 contents. The basic composition - 50
16 $\text{Sb}_2\text{O}_3 - 50\text{PbO}$ - was chosen in the range of minimum stability in order to make clear the effect
17 of additive concentration on glass stability. As shown in figure 8, a first result concerns T_g
18 that increases with In_2O_3 concentration.
19
20

21 Another set of glass samples was prepared with the general formula: $50 \text{Sb}_2\text{O}_3 - (50-x) \text{PbO} - x$
22 Me_2O_3 (Me= Al, Ga, In). Glass transition T_g increases quasi-linearly with Me_2O_3 addition.
23 Once again, larger T_g values are observed for cations with larger ionic radius.
24
25
26

27 Figure 10 reports the variation of the stability factor S as a function of Me_2O_3 concentration
28 for the $50 \text{Sb}_2\text{O}_3 - (50-x) \text{PbO} - x \text{Me}_2\text{O}_3$ glasses.
29

30 These curves suggest that Me_2O_3 addition has a stabilizing effect by comparison to the binary
31 glass. At first glance, glasses containing Ga content appear as the most stable ones. However
32 additional experiments should be implemented to confirm these observations: first, no data
33 were collected for Me_2O_3 concentrations between 5 and 10 mol %; and second, no stable glass
34 was obtained for In_2O_3 concentrations larger than 5 mol % (see fig. 3). Then one would
35 expect the sharp decrease of the stability factor beyond some threshold value that could be
36 found experimentally.
37
38
39
40

41 **3.4 Density**

42 The composition dependence of the density of the binary glass samples in the $\text{Sb}_2\text{O}_3 - \text{PbO}$
43 system is shown in fig 11.
44
45

46
47
48 As one could expect, density d decreases as lead oxide is replaced by antimony sesquioxide.
49 This change is approximately linear. Another set of density measurement has been
50 implemented in the ternary system with the following formula: $x\text{Sb}_2\text{O}_3 - (95-x) \text{PbO} - 5\text{Me}_2\text{O}_3$
51 (Me = Al, Ga, In). As shown in figure 12, density also decreases linearly with the substitution
52 of PbO by Sb_2O_3 .
53
54

55 **3.5 Microhardness**

56
57
58 Figure 13 shows the microhardness variation of the $50\text{Sb}_2\text{O}_3 - (50-x) \text{PbO} - x\text{Me}_2\text{O}_3$ (Me = Al,
59 Ga, In) glasses as a function of Me_2O_3 concentration. Microhardness increases with Me_2O_3
60
61
62
63
64
65

1 concentration. For the same oxide content microhardness increases according to the sequence:
2 Hv(Al)<Hv(Ga)<Hv(In)
3

4 Discussion 5

6 This study exemplifies the respective parts of the glass components. Antimony sesquioxide
7 Sb₂O₃ is clearly a vitrifying oxide. Even though the existence of pure vitreous Sb₂O₃ has been
8 for long a matter of discussion, the occurrence of numerous binary glasses with high Sb₂O₃
9 concentration confirms its glass forming ability. It complies with Zachariasen's rules[7]
10 insofar as it forms tetrahedra in the solid state that must be written SbO₃(LP), where LP is a
11 lone pair of s² electrons. In this way it offers similarities with phosphate groups PO₄ in which
12 one oxygen is non-bridging. The vitreous network is constructed from these SbO₃(LP)
13 tetrahedra, with up to three non-bridging oxygens.
14

15 Lead oxide PbO is known to have a dual role, depending on glass composition and also on the
16 nature of the other vitrifiers. Solid state chemistry teaches that Pb²⁺ commonly acts as a large
17 cation that leads to compounds isostructural with those obtained with Sr²⁺, Ba²⁺ or Eu²⁺.
18 Among other examples one may quote perovskite PbZrO₃ and fluorite-type PbF₂. In these
19 structures, coordination number is high: 12 in perovskite and 8 in fluorite [21]. Based on this
20 coordination and the corresponding size effect, divalent lead is considered as a modifier that
21 fills empty space within the vitreous network. This behavior is common at low PbO content.
22 However, at high concentrations, the structural behavior of Pb²⁺ is different and compares to
23 that of trivalent antimony. Its coordination number drops down while a lone pair of s²
24 electrons completes a smaller coordination polyhedron. This polyhedron typically consists of
25 4 oxygens and one lone pair. This makes the basis of the PbO structure. Then this PbO₄ group
26 can enter the vitreous network. Indeed there are numerous examples of glass compositions
27 with a very large content of lead oxide. In the Sb₂O₃-PbO binary system, there are two
28 different glass domains, the first one for large Sb₂O₃ concentrations and the second one when
29 lead is predominant. Not surprisingly characteristic temperatures reflect this situation (fig. 6):
30 less stable glasses are found in the intermediate composition range.
31

32 The optical quality of the glass samples is very sensitive to the redox conditions. There
33 are several redox couples that interact in glass melt: Sb³⁺/Sb⁵⁺, Pb²⁺/Pb⁴⁺, Pb⁰/Pb²⁺.
34 Equilibrium constants vary with temperature. In order to limit the formation of reduced
35 species, it is necessary to maintain an oxidizing atmosphere that can be provided by room
36 atmosphere. However, in some cases, longer melting – and fining- time are required. When
37 silica crucibles are used, this results in a larger contamination by silica. This drawback is
38 avoided with other crucible materials such as alumina.
39

40 The influence of the third component on thermal properties is unexpected. In classical
41 oxide glasses –silicates, phosphates, borates- glass transition temperature decreases as the
42 ionic radius of the modifying element increases: T_g is smaller when sodium is replaced by
43 potassium, rubidium or cesium. When network formers are incorporated, T_g variation is ruled
44 by the relative bond strength of the new element. For example, the Si/Ge substitution leads to
45 lower T_g's. In these glasses, the bond strength of aluminum vs. oxygen is much larger than
46 that of gallium and indium. However, for the same nominal composition, larger T_g is
47 observed with Ga₂O₃ and In₂O₃ (fig. 9). Then, it appears that bond strength is not the major
48 parameter to account for this observed variation. Rather changes in glass structure should be
49 considered. While these three cations –Al,Ga,In- are likely to enter the vitreous network, their
50 coordination number is expected to be 6. As a result, the number of non-bridging oxygens is
51 reduced, and consequently, glass transition temperature is lowered. This mechanism could
52
53
54
55
56
57
58
59
60
61
62
63
64
65

also explain the increase of microhardness with the incorporation of the Me_2O_3 oxides in the Sb_2O_3 - PbO binary glass (fig. 13).

Conclusion

The incorporation of trivalent oxides in the Sb_2O_3 - PbO binary glass has been studied. Characteristic temperatures, density and microhardness have been measured for binary glasses. The limits for glass formation have been defined by a set of systematic experiments in the Sb_2O_3 - PbO - Me_2O_3 ($\text{Me}=\text{Al}, \text{Ga}, \text{In}$) ternary systems. Up to 10 mol % Me_2O_3 oxide could enter glass composition. Thermal measurements show that characteristic temperatures increase with oxide addition. In the mean time, glass is less prone to devitrification. Glass transition temperature increases according to the sequence: $T_g(\text{Al}) < T_g(\text{Ga}) < T_g(\text{In})$. Microhardness variation is similar, and maximum values are observed for indium containing glasses. It is suggested that this unexpected variation occurs from the decrease of the number of non-bridging oxygens. This decrease could result from the 6 coordination number of the trivalent cations that take place in the vitreous network.

Acknowledgment

The authors would like to thanks PNE (Algerian program) for the financial support.

References

- [1] J.M. Fernández Navarro, *El Vidrio. Constitución, fabricación, propiedades*, Consejo Superior de Investigaciones Científicas, Madrid, 2003.
- [2] C. Moretti, English lead crystal. The Ravenscroft recipe and points not clear on the process of development of “flint” glass formulation, Proc. of the 16th Congress of the AIHV, London, 7–13 September 2003, 2005.
- [3] W.H. Dumbaugh, J.C. Lapp, *J. Am. Ceram. Soc.* 75 (1992) 2315-2326.
- [4] J.S. Wang, E.E. Vogel, Snitzer, *Opt. Mater* 3 (1994) 187-203.
- [5] B. Dubois, H. Aomi, J.J. Videau, J. Portier, Haggemuller, *Mater.Res Bull.* 19(10) (1984) 1317-1323.
- [6] R.E.de Araujo, C.B. de Araujo, G. Poirier, M. Poulain, Y. Messaddeq, *Appl. Phys. Lett* 81(2002) 4694-4696.
- [7] W.H Zachariasen, *J.Chem. Soc* 54(1932)3841
- [8] M.T. Soltani, A. Boutarfaia, R. Makhloufi, M. Poulain, *J. Phys. Chem. Solids* 64 (2003) 2307–2312
- [9] A. Winter, *Verres Réfract.*, 36 (2), 353-356 (1982)
- [10] Y. Taibi, M. Poulain, R. Lebullenger, L. Atoui, M. Legouera, *J Opt Adv Mat.* 11 (2009) 34 - 40
- [11] K. Nageswara Rao, N. Veeraiyah, *Ind. J. Phys.* 74A (2000) 37
- [12] M.R. Reddy, S.B. Raju, N. Veeraiyah, *J. Phys. Chem. Solids* 61 (2000) 1567.
- [13] P. Kantor, A. Revcolevschi, R. Collongues, *J. Mater. Sci.* 8 (1973) 1359.
- [14] H. Morikawa, J. Jegoudez, C. Mazieres, A. Revcolevschi, *J. Non-Cryst. Solids* 44 (1981) 107.
- [15] W.H. Dumbaugh, *Phys. Chem. Glasses* 27 (1986) 119.
- [16] J.E. Shelby, *J. Am. Ceram. Soc.* 71 (1988) C-254.
- [17] F. Miyaji, K. Tadanaga, T. Yoko, S. Sakka, *J. Non-Cryst.Solids* 139 (1992) 268.
- [18] K. Suzuya, C.-K. Loong, D.L. Price, B.C. Sales, L.A. Boatner, *J. Non-Cryst.Solids* 258 (1999) 48-56.

[19] M. Saad, M. Poulain, Mat. Sci. Forum 19&20 (1987) 11.

[20] A. Dietzel, Glastech. Ber., **22**(7), 41 (1968).

[21] Yet-Ming Chiang, Dunbar Birnie III, David Kingery, Physical Ceramics- Principles for Ceramic Science and Engineering, John Wiley (1997).

1
2
3
4
5
6
7
8
9
10
11
12
13
14
15
16
17
18
19
20
21
22
23
24
25
26
27
28
29
30
31
32
33
34
35
36
37
38
39
40
41
42
43
44
45
46
47
48
49
50
51
52
53
54
55
56
57
58
59
60
61
62
63
64
65

Figures of the manuscript :

INVESTIGATION AND PROPERTIES OF NOVEL LOW MELTING GLASSES IN
THE TERNARY SYSTEM Sb_2O_3 - PbO - Me_2O_3

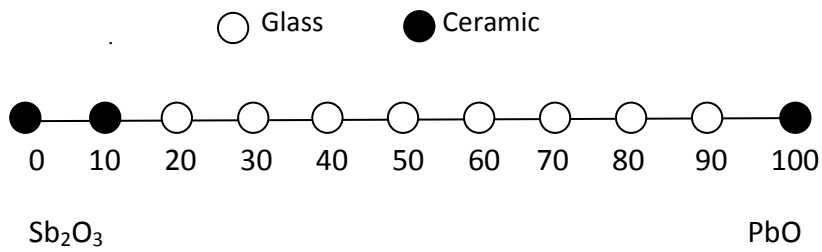


(fig 1)

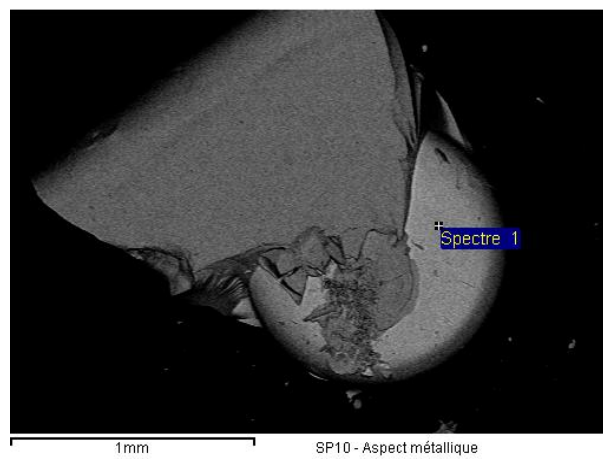
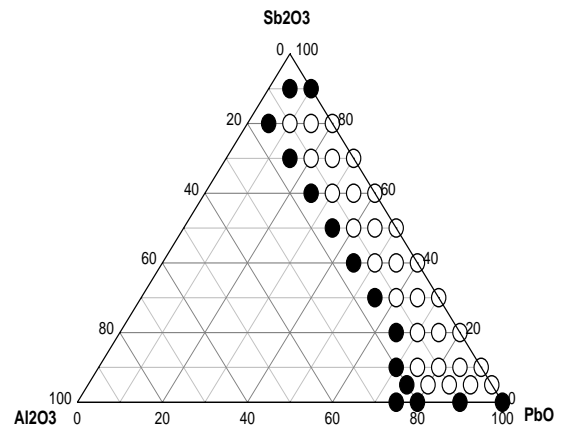
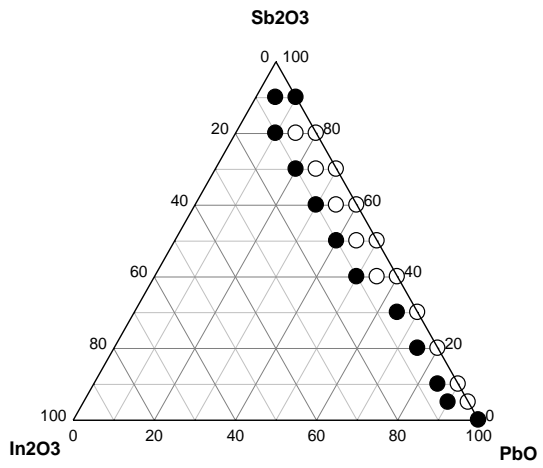
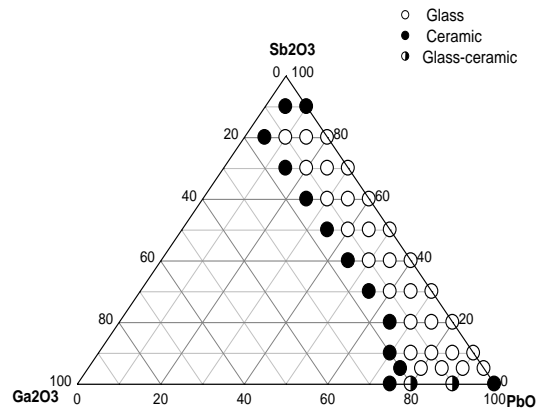


(fig 2)



These 3 diagrams belong to the same figure (figure 3)

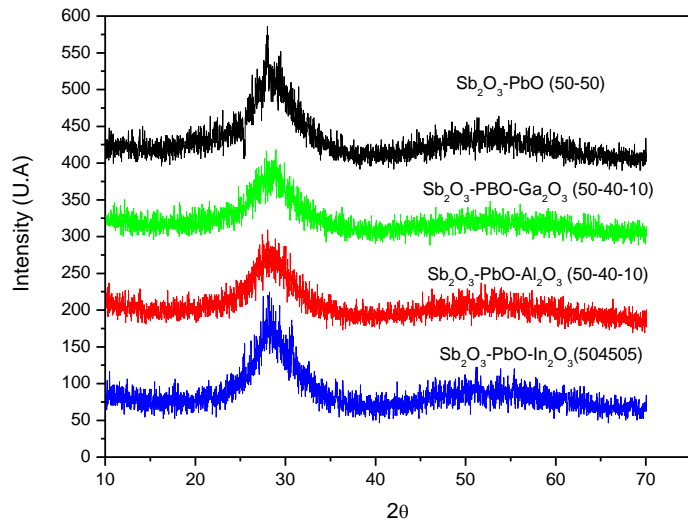


(Fig 4)

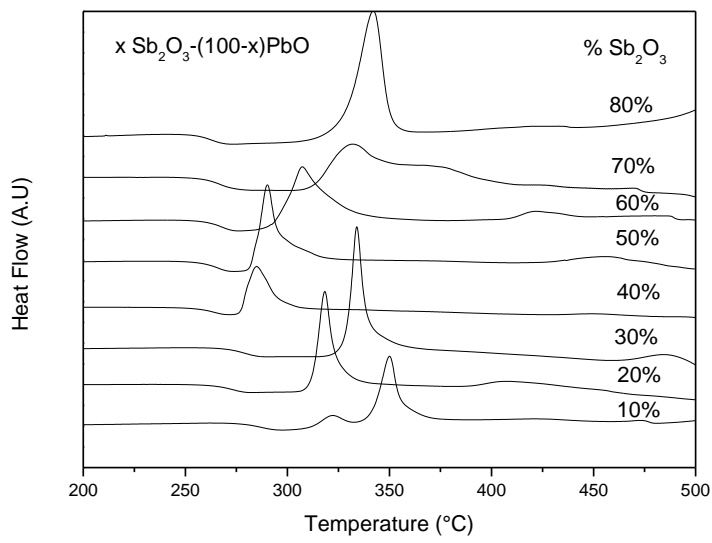


(fig 5)

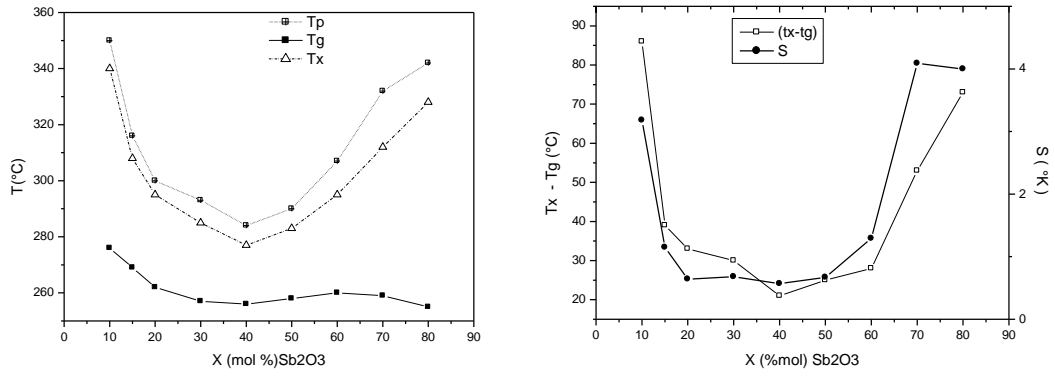


(Fig 6)

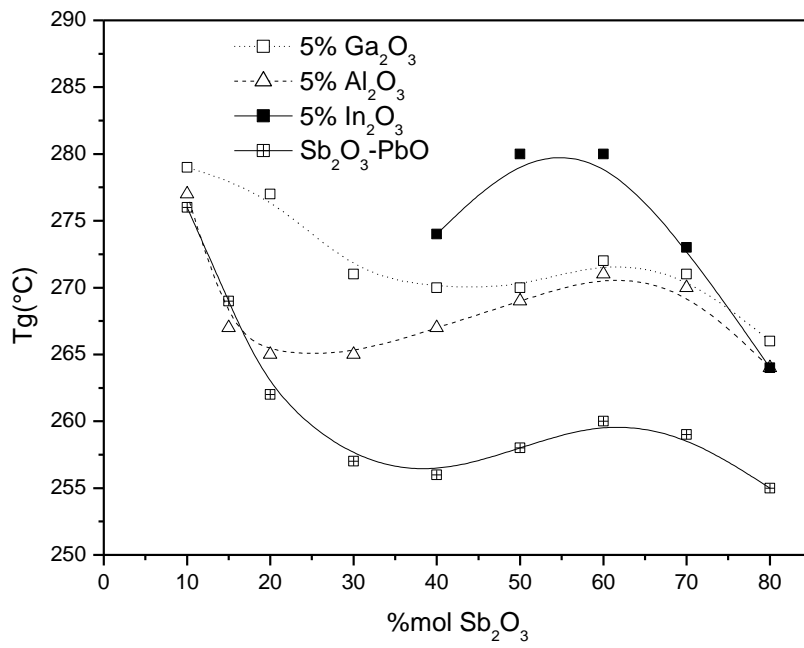


(Fig 7)

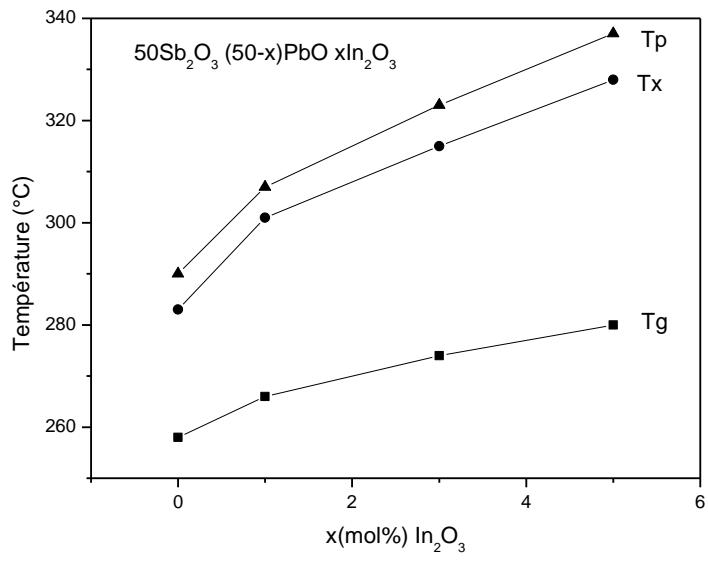


(fig 8)

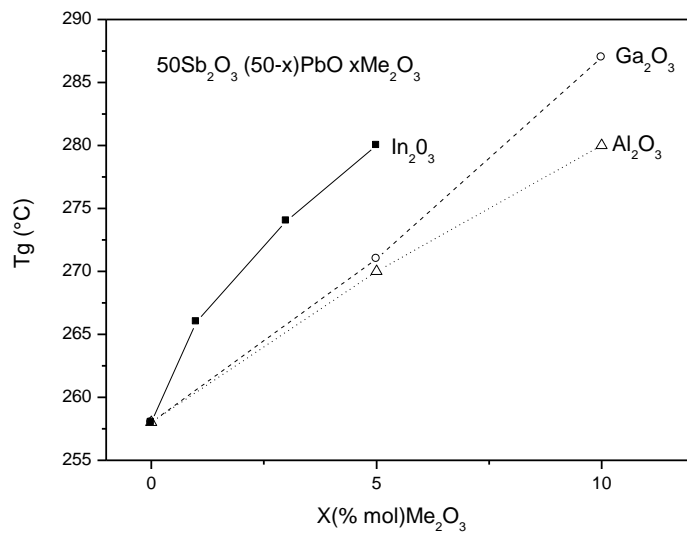


(fig 9)

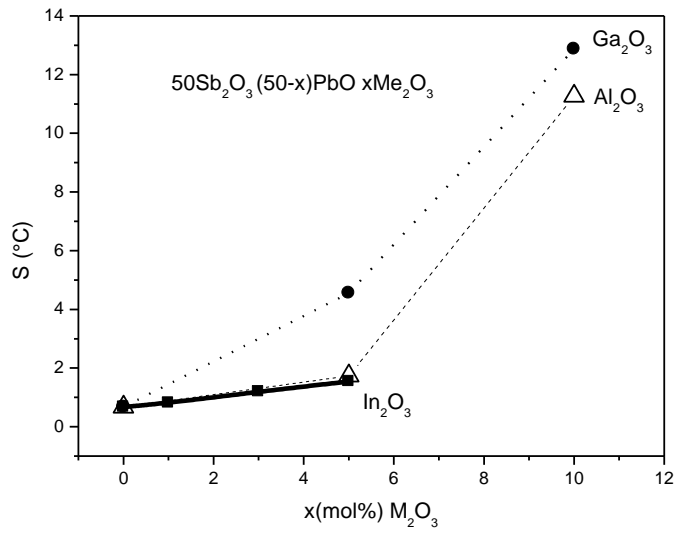


(fig 10)

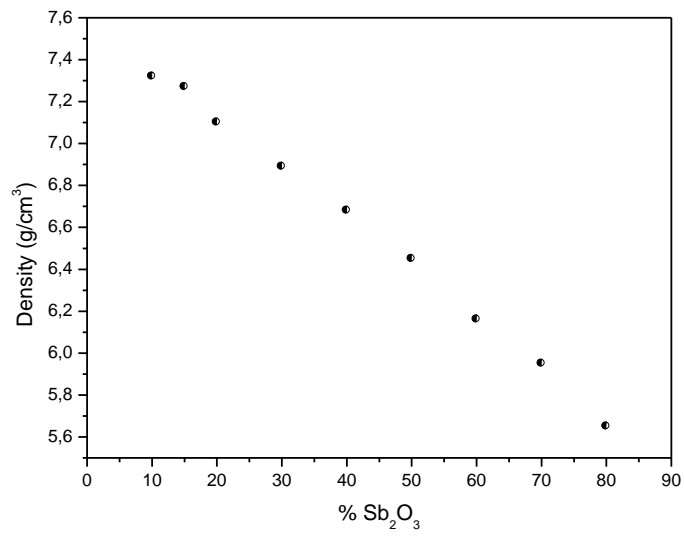


(fig 11)

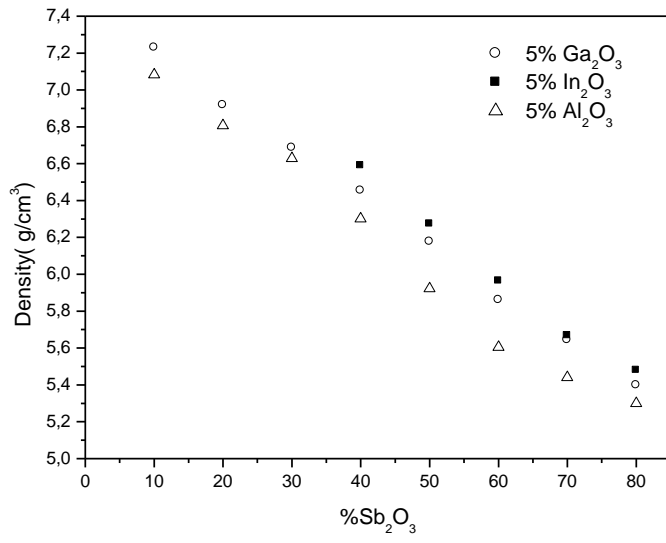


(fig 12)

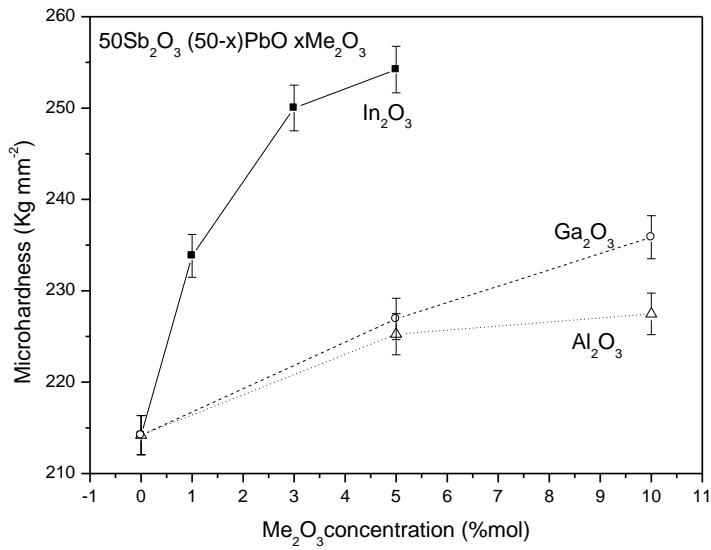


(fig 13)